engineering proceedings

MDPI

Proceeding Paper

Indoor Signal Strength Evaluation of the Orbcomm Low Earth Orbit Satellite Constellation †

Wout Van Uytsel *, Thomas Janssen, Maarten Weyn and Rafael Berkvens

Faculty of Applied Engineering, imec-IDLab, University of Antwerp, 2000 Antwerp, Belgium; thomas.janssen@uantwerpen.be (T.J.); maarten.weyn@uantwerpen.be (M.W.); rafael.berkvens@uantwerpen.be (R.B.)

* Correspondence: wout.vanuytsel@uantwerpen.be

† Presented at the European Navigation Conference 2024, Noordwijk, The Netherlands, 22–24 May 2024.

Abstract: In this connected world, communication in all kinds of complex environments is crucial. As a result, indoor satellite communication could enable many new applications and use cases. In this study, we explore the potential of Low Earth Orbit (LEO) satellites to provide indoor coverage. This is done by evaluating the signal strength of Orbcomm LEO satellite signals in multiple indoor environments within a suburban home. Starting from IQ samples, we developed an algorithm to calculate the Carrier-to-Noise Density Ratio (C/N0) as a key performance metric to compare environments when the Carrier-To-Noise Ratio (CNR) is above 0 dB. By utilizing a Software Defined Radio (SDR) in combination with this algorithm, we were able to evaluate the signal strength differences between environments. We found that the LEO satellite signals penetrated into every environment including the basement. The signals were even received with high signal strength in the attic, reaching values above 55 dB-Hz. Moreover, the signals were well received in every above-ground environment. Unsurprisingly, the satellite signals were received the weakest in the basement and only for a short duration of time.

Keywords: LEO; Orbcomm; signal strength; indoor satellite communication; LEO-PNT; satellite communication

check for updates

Academic Editor: Terry Moore

Published: 29 April 2025

Citation: Van Uytsel, W.; Janssen, T.; Weyn, M.; Berkvens, R. Indoor Signal Strength Evaluation of the Orbcomm Low Earth Orbit Satellite Constellation. *Eng. Proc.* **2025**, *88*, 39. https://doi.org/10.3390/engproc2025088039

Copyright: © 2025 by the authors. Licensee MDPI, Basel, Switzerland. This article is an open access article distributed under the terms and conditions of the Creative Commons Attribution (CC BY) license (https://creativecommons.org/licenses/by/4.0/).

1. Introduction

In the global economy, Low Earth Orbit (LEO) satellites are of increasing importance in asset tracking, vehicular navigation and emergency communication, among others. The main enabler for this is the decline in the cost of launching satellites into LEO, which plays a vital role in opening up this 'New Space' economy [1]. These launch costs have been steadily declining over the past decade, thus opening up new opportunities for companies to design, develop, and launch constellations.

Indoor signal coverage has always been challenging for higher-orbiting satellite constellations such as the Global Positioning System (GPS) [2]. This is due to the limited Power on Ground (PoG) provided by these satellites, which could lead to unreliable services and bad connectivity in indoor environments. LEO satellites could provide a solution to this problem, due to the shorter path the signal must travel to reach the User Equipment (UE) [3]. This indoor connectivity unmistakably could be used by a wide variety of applications such as asset tracking, vehicular navigation, and emergency communication [2]. Multiple LEO constellations are currently operational, which facilitates the possibility of conducting real-world experiments of the indoor signal strength [4]. Furthermore, calculating wall

material losses quickly becomes very difficult due to a large number of variables to take into account [2,5]. Therefore, in-situ measurements are the preferred method [2].

In this work, we provide a coverage analysis of different indoor environments for the Orbcomm satellite constellation. This constellation provides a downlink in the Very High Frequency (VHF) band, which could result in better indoor coverage. More specifically, the constellation utilizes a downlink frequency range of 137 MHz up to 138 MHz. Our contribution is (1) an assessment of the limits and possibilities of indoor coverage of Orbcomm LEO satellites, and (2) a quantification of how strong these Orbcomm satellite signals propagate into different indoor environments.

This paper is outlined as follows. Section 2 analyses similar, previously conducted studies on this topic. Section 3 provides an outline of the research methodology. Section 4 supplies the results in terms of coverage and Section 5 discusses these results. Finally, Section 6 draws the conclusion of the research.

2. Related Work

A limited amount of studies have been conducted on the topic of the indoor signal strength of LEO satellites. A few experiments have already been conducted using the Iridium constellation, which utilizes the L-band frequency (1610 MHz up to 1626.5 MHz) to transmit downlink packets [6,7]. However, higher frequencies experience significantly more wall attenuation than lower frequencies [5].

A first study simulated the differences in the Carrier-to-Noise Density Ratio (C/N_0) between LEO constellations and Medium Earth Orbit (MEO) constellations in an indoor environment. Ferre et al. have shown that in simulation, the indoor C/N_0 of LEO satellites is similar to the outdoor C/N_0 of Medium Earth Orbit satellites [8]. More specifically Starlink, OneWeb, and Kuiper, which are all situated in LEO, showed a similar indoor C/N_0 to the outdoor C/N_0 of the Galileo constellation which is situated in MEO. In the simulation the outdoor C/N_0 of Galileo is 24.9 dB–Hz, similar results were observed for Starlink, OneWeb and Kuiper in an indoor setting. More specifically, the Starlink constellation had an indoor C/N_0 of 23.1 dB–Hz, the OneWeb Constellation had a C/N_0 of 23.7 dB–Hz and Kuiper had a C/N_0 of 22.3 dB–Hz. To conduct this simulation, the QUAsi Deterministic RadIo channel GenerAtor (QuaDRiGa) framework was used in addition to MATLAB [9]. Furthermore, the frequencies used in the simulation matched with the real constellation frequencies as well as the antenna parameters [8]. The values put forward in this paper do deviate from what is commonly found in other papers. Specifically, the outdoor C/N_0 of GPS typically ranges between 30 dB–Hz and 50 dB–Hz which was not the case in this paper [7,10].

Second, a study by Reid et al. conducted real-life measurements of the C/N_0 of LEO satellites [6]. These experiments were performed in a 13-story office building. The experiment consisted of measuring the C/N_0 of Iridium Satellite Time and Location (STL) signals. Additionally, a GPS receiver was used to evaluate if the Ground Receiving Station (GRS) could use this MEO constellation to locate itself. The results of this study showed that even on the 13th floor the GPS signals could not penetrate inside well enough to determine the location. A minimum of four satellite signals are necessary to determine the location of the receiver and in this study, only one to two satellite signals arrived strong enough to decode. In contrast to the Iridium STL signals, which were received with high C/N_0 on the 13th floor. Moreover, the Iridium STL signals even arrived with high C/N_0 inside on the second floor. More specifically, these signals arrived with a C/N_0 between 45–55 dB–Hz [6].

A third and last study, similar to that of Reid et al., was conducted by Enge et al. They measured C/N_0 inside a metal container [7]. These measurements showed that the C/N_0

of the Iridium STL signals inside of the container were similar to that of GPS in an outdoor environment (±45 dB–Hz).

The above studies have shown the potential of indoor satellite communication from LEO. However, a more complete picture in terms of environments is needed to judge the feasibility. Hence, this work aims to analyze the received signal strength in different indoor rooms and floor levels.

3. Material and Methodology

We will analyze the signal strength in various outdoor and indoor environments. To evaluate the link quality, two parameters are commonly utilized. The first parameter is the Carrier-to-Noise Ratio $\left(\frac{C}{N}\right)$. Which is the ratio of carrier power over noise power in the channel [3]. This parameter is a good indicator of system performance and can be calculated as such [11]:

$$\left(\frac{C}{N}\right) = P_C - P_N \tag{1}$$

with $\left(\frac{C}{N}\right)$ in dB, P_C is the carrier power in dBW and P_N is the noise power in dBW [3]. The second commonly used parameter is the C/N_0 which is the ratio of carrier power to the noise power per unit bandwidth. To calculate the C/N_0 the following formula can be used [3]:

$$\left(\frac{C}{N_0}\right) = \left(\frac{C}{N}\right) + B_N \tag{2}$$

with C/N_0 in dB-Hz, $\left(\frac{C}{N}\right)$ in dB and B_N the bandwidth in dB-Hz.

3.1. Receiver Setup

To measure the signal power of Orbcomm satellites in different environments, we constructed a receiver, which consists of a Software Defined Radio (SDR) and an antenna connected via a one-meter coaxial cable. In what follows, we will further describe these components.

An SDR provides a flexible and versatile radio platform [12]. Previously, these physical layers were implemented in hardware, but hardware redesign can be time-consuming and costly. The SDR, by contrast, has the possibility to adapt to different protocols, bandwidths, as well as frequencies [13]. Furthermore, the data can easily be saved and post-processed. This makes it a great choice for this type of research. For this paper, the Ettus B210 was used which has the ability to receive signals between 70 MHz and 6 GHz and with a maximum bandwidth of up to 56 MHz. This SDR utilizes the AD9361 chip which is a high-performance transceiver [14]. The two receivers onboard feature a 12-bit resolution and a configurable gain between 0 and 74.5 dB. When the center frequency is set to 800 MHz, the Noise Figure (NF) is equal to 2 dB and the accuracy is ±2 dB [15]. The NF is not indicated for the frequency range that we utilize, therefore, this is the closest available value.

Two main factors should be taken into account when selecting a receiving antenna from the wide range of available options. First, the polarization of the transmitting antenna on the satellite should ideally match the polarization of the GRS antenna, otherwise, this will result in polarization losses. Second, the gain of the antenna should be taken into account. A high-gain antenna results in a stronger received signal but requires tracking the satellites, whereas an omnidirectional antenna does not require tracking [3,16].

For our setup, we selected an antenna which was optimal for receiving the Orbcomm constellation. This constellation utilizes a Right Hand Circular Polarized (RHCP) signal with downlink frequencies between 137 MHz and 138 MHz. Therefore, we selected the Diamond DPKE137 antenna, as shown in Figure 1. This antenna is a RHCP quadrifilar

helix antenna designed to receive this frequency band [17]. The quadrifilar helix antenna is an improved version of the regular helical antenna. Adding extra windings tightens the radiation pattern and minimizes sidelobes. Moreover, the quadrifilar helix antenna is more omnidirectional than the helical antenna [18].



Figure 1. The Diamond DPKE137 RHCP quadrifilar helix antenna in an outdoor environment.

3.2. The Orbcomm Constellation

Since 1995, the Orbcomm satellite constellation has provided users with the ability to transmit and receive information in remote areas. Multiple sectors leverage this constellation, such as the maritime sector which uses the Orbcomm satellite constellation to transmit and receive Automatic Identification System (AIS) data. Furthermore, in the transport sector, the constellation is used to track and get status updates from vehicles [19].

The Orbcomm system consists of UE, a space segment, and Earth stations. The space segment consists of two generations of satellites, namely, Orbcomm Generation 1 (OG1) and Orbcomm Generation 2 (OG2). The characteristics of the constellation as they were designed can be found in Table 1.

Table 1. The key characteristics of the Orbcomm OG1 and OG2 constellation [4,20].

Generation	Plane Designation	Number of Orbital Planes	Inclination	Altitude	Planned no. of Satellites
OG1	A, B, C, D	4	45°	825 km	8 in each plane
OG1	E	1	0°	1000 km	7
OG1	F	1	70°	775 km	4
OG1	G	1	108°	830 km	4
OG2	?	3	47°	715 km	4 in each plane
OG2	?	1	47°	715 km	3

The Orbcomm space segment functions as a link between the user and a gateway station on Earth. The satellites transmit a constant downlink signal that user devices can tune into. On this downlink channel, user devices can find the active uplink channels of that satellite. The user device can use these channels to transmit data to the satellite, which in turn relays it to the Earth gateway station. The downlink frequencies are positioned between 137 MHz and 138 MHz and the antenna subsystem of these Orbcomm satellites consists of a RHCP quadrifilar helix antenna which transmits with an Effective Isotropic Radiated Power (EIRP) of 12 dBW [20].

The 137–138 MHz band is not exclusively used by Orbcomm for downlink communication. Multiple meteorological satellites use this frequency range to communicate,

for instance, the National Oceanic and Atmospheric Administration (NOAA) satellites have multiple downlink channels in this band [20]. The band is also used by the recently launched SpaceBEE constellation [4]. Despite the shared use of this frequency band, there is no overlap between these systems. They each use their own well-defined frequency ranges within this band [20].

Currently, the Orbcomm constellation does not exactly meet the specifications of Table 1. At the time of writing, the actual OG1 constellation consist of 22 functional satellites and one semi-operational satellite. Most of the OG1 satellites are currently also in a lower orbit which is between 750 km and 790 km [21]. The OG2 constellation consists of 12 functional satellites [21]. Some confusion surrounds this subject since at the moment, even the official Orbcomm website does not correctly display which satellites are operational [19]. However, 'operational' does not necessarily mean that the satellite is actively transmitting. During the measurement campaign, very few signals from OG1 satellites were received. This is in contrast with the operational OG2 satellites, which are all actively transmitting.

3.3. Data Processing

In this paper, multiple satellite passes were recorded. These recordings were scheduled in SDR Console, a software program used to record the incoming IQ data. The recording starts once a satellite reaches an elevation angle of 5° and continues as long as the satellite remains at an elevation angle above 5°. This window of recording was calculated with the help of Two Line Element (TLE) files. These publicly available files precisely define the current orbit of satellites and can be used to predict the future trajectory [21]. In practice, this resulted in recording fragments of about 12–15 min. The sample rate of the SDR was set to 1 MHz and captured the full Orbcomm downlink spectrum from 137 MHz to 138 MHz. After recording the satellite passes, the data is processed offline. The processing flow is illustrated in Figure 2. Firstly, the recording gets split into 1-s fragments and fed into the processing algorithm where it is windowed to prevent spectral leakage [22]. After this, the conversion to the frequency domain is made by applying a Fast Fourier Transform (FFT). The zero frequency component is shifted to the center and the absolute value is calculated. Then, we make the conversion to the power spectrum [22]. To calculate P_N, first, the average noise power per bin is calculated. This is done by sorting the bins and discarding the highest bins that match the active Orbcomm channels and DC bin. Subsequently, the noise density is calculated. To get an estimate of the noise power in the Orbcomm channel, the noise density is multiplied by the bandwidth. Following this, the conversion to dBW is made. To calculate P_C, the peak bin within an Orbcomm channel is identified and the surrounding bins are summed. Afterwards, the conversion to dBW is made. Finally, to calculate the C/N and C/N_0 the formulas of Section 3 are employed.

3.4. Environmental Influences on Measurements

Due to external influences, measurements at different points in time or at different locations will never be exactly the same. One of the most significant influences is interference. In an indoor environment, many electrical devices are present and most of them emit some sort of Radio Frequency Interference (RFI). Additionally, the ionospheric Total Electron Content (TEC) changes over time and this results in different scintillation effects. Ionospheric scintillation results in rapid fluctuations of the amplitude and phase which is caused by electron density irregularities and has been observed the most on VHF frequencies [3].

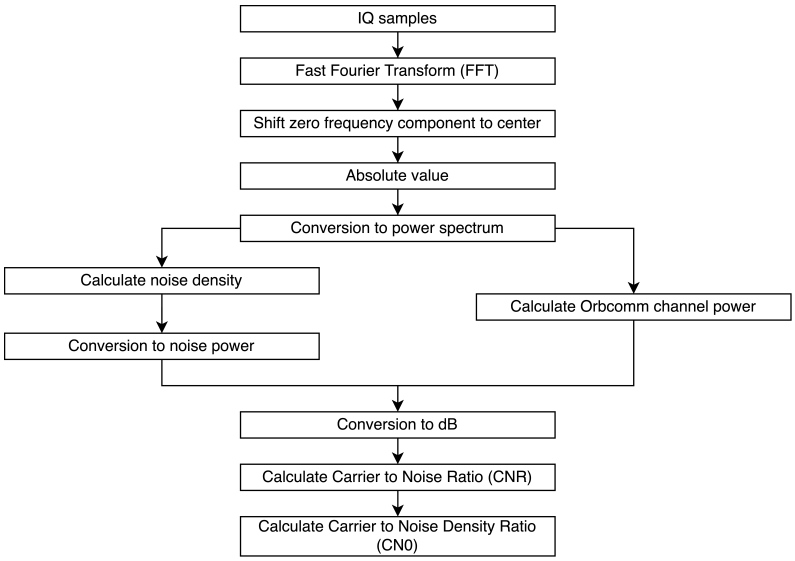

Figure 2. Flowchart of employed processing algorithm to transform incoming IQ samples to C/N_0 of a selected Orbcomm downlink channel.

4. Results

The primary objective of this research is to assess how well LEO satellite signals penetrate indoor environments. To this end, we performed multiple measurements in a variety of indoor environments. The C/N_0 was employed as the key performance metric to compare different environments with each other.

4.1. Outdoor

In order to obtain a point of reference, multiple outdoor measurements were performed. The outdoor measurements were performed in a garden located in a suburban area. Some fading was induced by multiple trees, a shed, neighboring houses, and others. Figure 3 shows a clear relation between the elevation angle and the C/N_0. A higher elevation angle implies a stronger received signal. This must be attributed mainly to the shorter range that the signal has to travel and to the fact that the antenna has a higher gain for higher elevation angles. For elevation angles above 40°, the outdoor C/N_0 peaked at almost 70 dB–Hz. Due to the geographical location where the measurements took place, no satellite passes were recorded with a maximum elevation angle above 55°. Furthermore, satellite passes with lower elevation angles were still well received, such as the pass with a max elevation angle of 5.5° as seen in Figure 3.

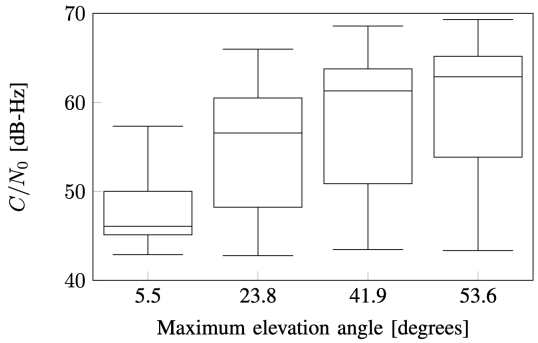

Figure 3. Comparison of signal strength of multiple outdoor satellite passes in a suburban garden with different maximum elevation angles.

4.2. Indoor Measurements

After having established a baseline in the outdoor environment, the measurement setup was moved indoors. The indoor environments are described in detail in the following subsections and a comparison can be found in Figure 4, which shows data from two satellite passes per environment. Each environment contains one satellite pass in the elevation angle range of 20° and 40°.

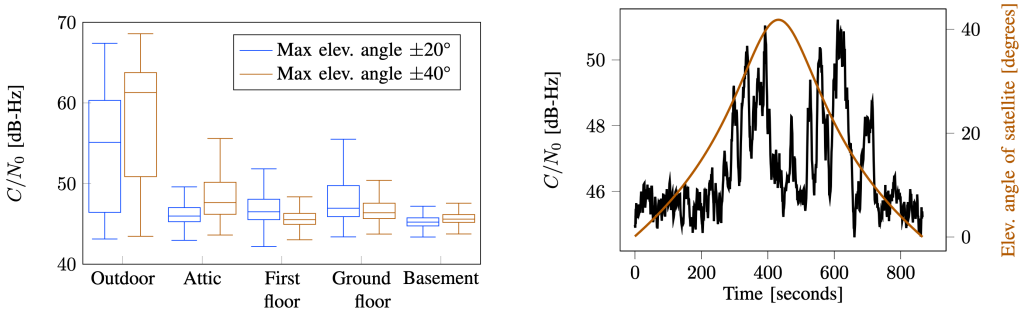

Figure 4. These figures illustrate the Orbcomm indoor signal strength in various environments. (**a**) Comparison. of Orbcomm satellite signal strength across various environments. Each boxplot depicts the signal strength of one satellite pass. (**b**) The C/N_0 of FM116 in the attic with a maximum elevation angle of 41.8°. A 5-second moving average filter was applied to the C/N_0 data.

4.2.1. Attic

The attic is located under a tiled roof which is inclined at 50°. This is the 3rd level of the house. Its insulation consists of 25 cm of glass wool. No windows through which the signal could potentially propagate were present in this room. Satellite signals in this room were received rather strongly. In a total of 20 satellite passes, the highest received C/N_0 was 56.9 dB−Hz. Furthermore, all of the 20 passes were received. Notably, multiple satellite passes showed similar patterns as seen in Figure 4. When the satellite reaches its maximum elevation angle, the signal strength decreases significantly. This pattern was present in multiple satellite passes recorded in the attic. Lastly, when analyzing Figure 4 it can be observed that the signals are still well received in this room even lower elevation angle passes reached a C/N_0 of up to 50 dB-Hz.

4.2.2. First Floor

The outer wall of the first floor consists of a layer of bricks, a layer of hollow clay bricks, and insulation in total measuring 30 cm. The slabs between the attic and first floor consist of reinforced concrete measuring 30 cm. Additionally, two small windows were present in this room. The signal strength in this room was the lowest of all above-ground rooms, reaching a maximum value of 55.6 dB−Hz in a total of 13 satellite passes. Nonetheless, all satellite passes were received. Surprisingly, in Figure 4 the satellite pass with the lower elevation angle was received more strongly than the satellite pass with the higher maximum elevation angle.

4.2.3. Ground Floor

The ground floor measurements were performed in a living room with multiple large windows. The outer wall consists of the same materials as on the first floor. Satellite signals on this floor were still well received at lower elevation angles. When satellites reached their maximum elevation angle, the signal showed a large decline in signal strength similar to the pattern seen in the attic. Noteworthy is that a higher elevation angle did not imply a higher signal strength in this location, which can be observed in Figure 4.

4.2.4. Basement

The basement walls are constructed of 30 cm thick concrete blocks. Furthermore, the slabs between the basement and the ground floor consist of reinforced concrete with a thickness of 34 cm. Remarkably, the Orbcomm satellite signals propagated into the basement. Nevertheless, it should be noted that the signals arrived with very little power and were only briefly visible. Furthermore, only 80% of the satellite passes were received. When analyzing Figure 4, the mean value was the lowest of all rooms.

5. Discussion

In this study, we found that the Orbcomm satellite signals propagated into all rooms of a suburban home. We compared and quantified signal strength in various environments, the results of which are summarized in Figure 4, illustrating the differences between the environments.

When examining the results from the outdoor measurements, a clear correlation between elevation angle and signal strength is present, which is to be expected. This can be observed in Figure 3. Despite the less-than-ideal conditions in the suburban environment, the signal was still received remarkably strong. The indoor signal strength is notably weaker. In the attic, the strongest signals were received out of all indoor environments. When comparing the 40° maximum elevation angle range of the attic to the outdoor measurements, the peak adjacent values are 13 dB−Hz lower. Similarly, the median is 13.6 dB−Hz lower. When analyzing the median of the other rooms, it can be observed that the first floor is 15.8 dB−Hz below the outdoor median and the ground floor 14.9 dB−Hz below the outdoor median. Finally, the median C/N_0 of the basement is 15.7 dB−Hz below the outdoor median. Remarkable is that the median C/N_0 of the ground floor at low elevation angles is higher than the one of the first floor, which might be due to the large windows. Another aspect to consider in indoor environments is that a higher elevation angle does not necessarily imply a higher signal strength, as is illustrated in Figure 4. In an indoor environment, material attenuation also plays a significant role in link performance. The attenuation is influenced by the elevation angle but also the azimuth angle of the satellite.

When comparing our work to the one conducted by Reid et al., some similarities and differences can be identified. Reid et al. also conducted real-life measurements of the C/N_0. However, these measurements were of Iridium satellites inside an office building. The C/N_0 results varied between 45 and 60 dB−Hz on the higher floor levels and between 45 and 55 dB−Hz on the lower floor levels [6]. It is important to note a significant distinction between the study by Reid et al. and the present study. Specifically, this work utilizes the Orbcomm satellite constellation, which operates in the VHF frequency range and has an EIRP of 12 dBW [20]. This differs from the Iridium constellation used by Reid et al., which utilizes a bursty L-Band downlink with an EIRP between 10.7 dBW and 27.1 dBW [4]. Therefore, some differences in results are to be expected. Nonetheless, this study indicates that the Orbcomm constellation results in similar C/N_0 values in the attic and on the ground floor as the Iridium constellation on the lower floors of an office building.

Furthermore, when comparing our C/N_0 results to those of GNSS, a distinctly higher C/N_0 can be observed from the Orbcomm constellation. The C/N_0 of GPS in an outdoor environment is approximately 45 dB−Hz [7], whereas the Orbcomm satellites reach a peak C/N_0 of approximately 70 dB−Hz in an outdoor environment. Furthermore, the Orbcomm LEO satellite signals exhibit high C/N_0 indoors even in comparison to outdoor GPS signals, reaching higher values as GPS in every location. However, it should be noted that in this study, we were unable to detect signals with a CNR below 0 dB. Thus, the lowest value we were able to detect was 43.97 dB−Hz.

6. Conclusions

The aim of this research was to evaluate the indoor coverage of Orbcomm satellites within a suburban setting. These satellites operate in LEO and transmit on the VHF band. By conducting multiple outdoor and indoor measurements, we examined the variations in signal strength across different environments. More specifically, the attic, the first floor, the ground floor, the basement and the garden were evaluated. Undoubtedly, the outdoor satellite signals were most strongly received. Furthermore, a clear correlation between a higher elevation angle and a higher signal strength was present. In an indoor setting, the satellite signals were received most strongly in the attic. However, a substantial difference in signal strength between outdoor and indoor was noted. Furthermore, similar signal strengths were observed on the above-ground floors. Notably, the Orbcomm satellite signals were received in the basement, which is constructed out of thick concrete walls and slabs, albeit with low power and only for a short duration of time.

Overall, this study proves that the Orbcomm satellite signals penetrate deeply indoors. The signals even arrived with high carrier-to-noise density ratio in multiple environments. The high Power on Ground highlights the feasibility of indoor satellite communication, which is simply not possible with the current implementation of Global Navigation Satellite Systems (GNSS) in MEO. Therefore, along with the declining costs associated with launching them, LEO satellites offer an interesting opportunity for future indoor satellite communication and navigation applications.

Author Contributions: Methodology, software, measurements, writing, and analysis, W.V.U.; conceptualization, writing, and validation, T.J.; supervision, and writing, M.W.; supervision, and writing, R.B. All authors have read and agreed to the published version of the manuscript.

Funding: This research received no external funding.

Institutional Review Board Statement: Not applicable.

Informed Consent Statement: Not applicable.

Data Availability Statement: The data used for this study is available upon request. Due to the large size and privacy concerns the data is not publicly available.

Conflicts of Interest: The authors declare no conflicts of interest.

References

1. Jones, H.W. The Recent Large Reduction in Space Launch Cost. In Proceedings of the 48th International Conference on Environmental Systems, Albuquerque, NM, USA, 8–12 July 2018; p. 81.
2. Lachapelle, G. GNSS Indoor Location Technologies. *J. Glob. Position. Syst.* **2004**, *3*, 2–11. [CrossRef]
3. Ippolito, L.J. *Satellite Communications Systems Engineering: Atmospheric Effects, Satellite Link Design and System Performance*; John Wiley & Sons: Hoboken, NJ, USA, 2008; pp. 1–376. [CrossRef]
4. Federal Communications Commission. *FCC International Bureau Filings*; Technical Report; FCC: Washington, DC, USA, 2023.
5. ITU-R—Radiocommunication Sector of ITU. Recommendation ITU-R P.2040-1: Effects of Building Materials and Structures on Radiowave Propagation Above About 100 MHz. *Recomm. ITU-R P.2040* 2015; p. 7. Available online: https://www.itu.int/rec/R-REC-P.2040/en (accessed on 23 April 2025).
6. Press, I.; Spurgeon, S. *Position, Navigation, and Timing Technologies in the 21st Century*; Institute of Electrical and Electronics Engineers: Piscataway, NJ, USA, 2020. [CrossRef]
7. Enge, P.; Ferrell, B.; Bennett, J.; Whelan, D.; Gutt, G.; Lawrence, D. Orbital Diversity for Satellite Navigation. In Proceedings of the 25th International Technical Meeting of the Satellite Division of The Institute of Navigation (ION GNSS 2012), Nashville, TN, USA, 17–21 September 2012; pp. 3834–3846.
8. Ferre, R.M.; Lohan, E.S.; Kuusniemi, H.; Praks, J.; Kaasalainen, S.; Pinell, C.; Elsanhoury, M. Is LEO-Based Positioning with Mega-Constellations the Answer for Future Equal Access Localization? *IEEE Commun. Mag.* **2022**, *60*, 40–46. [CrossRef]
9. Jaeckel, S.; Raschkowski, L.; Borner, K.; Thiele, L. QuaDRiGa: A 3-D multi-cell channel model with time evolution for enabling virtual field trials. *IEEE Trans. Antennas Propag.* **2014**, *62*, 3242–3256. [CrossRef]

10. Bhuiyan, M.Z.H.; Soderholm, S.; Thombre, S.; Ruotsalainen, L.; Kirkko-Jaakkola, M.; Kuusniemi, H. Performance evaluation of carrier-to-noise density ratio estimation techniques for BeiDou Bl signal. In Proceedings of the 2014 Ubiquitous Positioning Indoor Navigation and Location Based Service, UPINLBS 2014—Conference Proceedings, Corpus Christi, TX, USA, 20–21 November 2014; pp. 19–25. [CrossRef]
11. Joseph, A. Signal and Noise Paths from Antenna to Receiver. *InsideGNSS* November/December 2010; pp. 20–25. Available online: https://insidegnss.com/measuring-gnss-signal-strength/ (accessed on 23 April 2025).
12. Ulversoy, T. Software defined radio: Challenges and opportunities. *IEEE Commun. Surv. Tutorials* **2010**, *12*, 531–550. [CrossRef]
13. Bosco, M.; Tortora, P.; Cinarelli, D. Alma Mater Ground Station transceiver: A software defined radio for satellite communications. In Proceedings of the 2014 IEEE International Workshop on Metrology for Aerospace, MetroAeroSpace 2014-Proceedings, Benevento, Italy, 29–30 May 2014; pp. 549–554. [CrossRef]
14. Ettus Research. USRP B210, 2023. Available online: https://www.ettus.com/all-products/ub210-kit/ (accessed on 4 February 2023).
15. Analog Devices. AD9361 Datasheet. 2016. Available online: https://www.analog.com/en/products/ad9361.html (accessed on 14 February 2023).
16. Straw, R.D. *The ARRL Antenna Book*; Amer Radio Relay League: Newington, CT, USA, 2007; p. 1091, ISBN 978-1-62595-114-4.
17. Diamond Antenna. 2023. Available online: https://www.diamondantenna.net/ (accessed on 14 January 2023).
18. Slade, B. *The Basics of Quadrifilar Helix Antennas*; Technical Article; Orban Microwave Inc.: Leuven, Belgium, 2015. Available online: https://www.researchgate.net/profile/George-Slade-2/publication/275828209_The_Basics_of_Quadrifilar_Helix_Antennas/links/5547694f0cf249186bb0f455/The-Basics-of-Quadrifilar-Helix-Antennas.pdf (accessed on 5 March 2023).
19. ORBCOMM. *Industrial IoT and M2M Tracking, Monitoring and Control Solutions*; ORBCOMM: Rochelle Park, NJ, USA, 2023.
20. Reid, S.; Burdett Director, R.; Lord, M.; Rudd, T. A80TD0008-Revision G ORBCOMM System Overview. 2001. Available online: https://ctu.gov.cz/sites/default/files/cs/download/oznamene_typy_rozhrani/orbcomm-rozhrani_02_06_2010.pdf (accessed on 18 January 2023).
21. Kelso, T.S. CelesTrak: A New Way to Obtain GP Data (aka TLEs), 2023. Available online: https://celestrak.org/NORAD/documentation/gp-data-formats.php (accessed on 28 January 2023).
22. Scholl, S. *Exact Signal Measurements Using FFT Analysis*; Microelectronic Systems Design Research Group; 2016; pp. 1–10. Available online: https://kluedo.ub.rptu.de/frontdoor/deliver/index/docId/4293/file/exact_fft_measurements.pdf (accessed on 2 February 2023).

Disclaimer/Publisher's Note: The statements, opinions and data contained in all publications are solely those of the individual author(s) and contributor(s) and not of MDPI and/or the editor(s). MDPI and/or the editor(s) disclaim responsibility for any injury to people or property resulting from any ideas, methods, instructions or products referred to in the content.